Smart Structures and Systems, *Vol. 16, No. 3 (2015) 459-478*
DOI: http://dx.doi.org/10.12989/sss.2015.16.3.459

Design of a TMD solution to mitigate wind-induced local vibrations in an existing timber footbridge

Daniele Bortoluzzi[*1], Sara Casciati[2a], Lorenzo Elia[1b] and Lucia Faravelli[1a]

[1]*Department of Civil Engineering and Architecture, University of Pavia, Via Ferrata 3, 27100 Pavia (PV), Italy*
[2]*Department of Civil Engineering and Architecture, University of Catania at Siracusa, P.za Federico di Svevia, 96100 Siracusa, Italy*

(Received November 18, 2014, Revised December 20, 2014, Accepted December 28, 2014)

Abstract. The design of a passive control solution based on tuned mass dampers (TMD's) requires the estimation of the actual masses involved in the undesired vibration. This task may result not so straightforward as expected when the vibration resides in subsets of different structural components. This occurs, for instance, when the goal is to damp out vibrations on stays. The theoretical aspects are first discussed and a design process is formulated. For sake of exemplification, a multiple TMD's configurations is eventually conceived for an existing timber footbridge located in the municipality of Trasaghis (North-Eastern Italy). The bridge span is 83 m and the deck width is 3.82 m.

Keywords: footbridges; passive control; tuned mass damper; vibration mitigation; wind load

1. Introduction

The coupled use of timber (Giordano *et al.* 2009, Thelandersson and Larsen 2003 and Casciati and Domaneschi 2007) and steel structural elements is becoming common in Europe, especially when landscape architecture is concerned, as in the neighborhood of mountain villages. Footbridges represent a class of structural systems where such a materials coupling can be conveniently applied.

As well documented in the technical literature (see Sétra 2006 and Reynders *et al.* 2010, among others), the design of footbridges requires to pay special attention to the vibration aspects, which could easily produce discomfort to the users. Several passive and semi-active/active solutions were proposed in order to control such vibrations (the reader is referred to Casado *et al.* 2013 Moutinho *et al.* 2011, Diaz *et al.* 2012, Occhiuzzi *et al.* 2008, among others).

Cables are often met in the structural skeleton either for cable-stayed or for suspension architecture. If the purpose is to control cable vibrations alone, then it is known that viscous dampers provide a very efficient solution for these members. However, when the cables are replaced by tubular elements, their modest vibration amplitude makes these dampers ineffective.

∗Corresponding author, Ph.D., E-mail: daniele.bortoluzzi@unipv.it
[a] Professor, E-mail: sacasci@unict.it - lucia@dipmec.unipv.it
[b] Ph.D. Student, E-mail: lorenzo.elia@unipv.it

http://www.techno-press.org/?journal=sss&subpage=8 ISSN: 1738-1584 (Print), 1738-1991 (Online)

The passive control alternative is the adoption of tuned mass dampers (TMD) designed to contrast the local vibrations interesting a limited subset of masses.

This is the case approached in the present study, which is focused on the design of a suitable tuned mass damper system targeted to mitigate local, rather than global, oscillations induced by the wind action. Despite their localized nature, these oscillations can cause discomfort to the users, i.e., the crossing pedestrians. After a discussion of the problem in general terms, the reasoning is exemplified by considering a 83 m-span existing timber footbridge (Bortoluzzi *et al.* 2013a and Bortoluzzi *et al.* 2013b), for which the modelling is carried out based on the results of a series of in situ experimental campaigns. The footbridge with a simple static scheme was designed according to the national structural code. However, being the bridge located in a quite windy canyon , its low structural damping does not prevent the users from feeling the vibrations.

2. Problem formulation

The wind action is regarded as the excitation whose induced vibration must be mitigated. It is worth noting that, for footbridges, the so called “human induced vibrations” caused by the pedestrian crossing may also be significant, but this aspect is the object of further studies, which are still in progress for the considered footbridge.

The Finite Element Model (FEM) of the structural system is developed within the Mentat-Marc (www.mscsoftware.com) software environment by paying careful attention to all the details reported in the technical design documents. In particular, those associated with the selected materials are crucial in representing the correct footbridge dynamics, especially when the mechanical behavior of the wood material is modelled (Casciati and Domaneschi 2007).

By the FEM discretization, the original system of partial differential equations in space and time coordinates is managed to become a system of ordinary differential equations in the time variable. The discretization yields to write the equations governing the system dynamics in a standard matrix form

$$\mathbf{M}\mathbf{x}''(t) + \mathbf{C}\mathbf{x}'(t) + \mathbf{K}\ \mathbf{x}(t) = \mathbf{f}(t) \tag{1}$$

where **M**, **C** and **K** are the mass, damping, and stiffness matrices, respectively; **x** is the vector of the node generalized displacements, **f** the vector of nodal forces; *t* denotes the time, and a “prime” the time derivative.

2.1 Tuned mass dampers

A common solution in order to mitigate the vibrations consists of introducing a tuned mass damper (TMD) system, composed by one or more devices, each of them hung in a suitable position. The design of a TMD is a well-established topic for a single degree of freedom (SDOF) primary system, while for a multi degrees of freedom (MDOF’s) system the driving concept can be found in Rana and Soong (1998). The reader is also referred to Soong and Dargush (2007), Abe and Fujino (1994), Abe and Igusa (1995), Bandivadekar and Jangid (2012) and Casciati and Giuliano (2009).

The installation of the tuned mass dampers result in additional forces at the given locations (Soong and Dargush 2007) which modify the equations of motion as follows

$$\mathbf{Mx}''(t)+\mathbf{Cx}'(t)+\mathbf{Kx}(t)=\mathbf{f}(t)+\mathbf{T}\left[\mathbf{cz}'(t)+\mathbf{kz}(t)\right], \tag{2}$$

where **T** is a topological matrix, while the matrices **c** and **k** contain, for each equally designed TMD, the damping coefficient c and the stiffness k. The variable z is the relative displacement of the added mass of a single TMD at its anchorage point, and is governed by the following relationship:

$$mz''(t)+cz'(t)+Kz(t)=-mx''(t), \tag{3}$$

where m is the added mass, and x is the displacement of the hanging point in the direction of the TMD degree of freedom z.

2.2 The standard design of a single TMD device

The single tuned mass device is defined by the tuning frequency and the added mass, or better the ratio μ between this secondary mass and the primary one, for a SDOF primary system. The two parameters c and k in Eq. (3) depend on μ through relations obtained by some optimization criteria (Soong and Dargush, 2007, Abe and Fujino 1994, Abe and Igusa 1995, Bandivadekar and Jangid 2012 and Casciati and Giuliano 2009).

A first extension to MDOF's primary systems was developed for the design of TMD devices in frames with lumped masses at the stories (Soong and Dargush 2007). Let N be the number of degrees-of-freedom of a damped structure. If a single TMD is installed in correspondence to the j-th DOF, the equations of motion can be written as

$$Mx''(t)+Cx'(t)+Kx(t)=f(t)+\delta_j\left[c_j z'(t)+k_j z(t)\right], \tag{4}$$

where δ_j is a diagonal matrix of Kronecker indexes. These equations have to be coupled with Eq. (3) where all the coefficients come with the index j. Furthermore, if the TMD is to be designed for the i-th structural mode with modal properties M_i, K_i and C_i, the design problem is essentially similar to that of designing a TMD for a SDOF structure, since it can be formulated by expressing the displacements in terms of the modal coordinate $y(t)$. The resulting modal equation is

$$M_i y''(t)+C_i y'(t)+K_i x(t)=\Phi_i^T\left\{f(t)+\delta_j\left[c_j z'(t)+k_j z(t)\right]\right\}, \tag{5}$$

being Φ_i the eigenvector associated to the i-th mode. Note that z is a relative displacement, i.e., it is computed as the difference between the displacement of the added mass DOF and the displacement of the anchorage DOF. However, if the structure's i-th mode shape vector is normalized with respect to its j-th element, which corresponds to the TMD location, Φ_{ij} becomes unity and the reference DOF displacement, which appears in z, coincides with $y(t)$. Thus, under this normalization condition, the design of a MDOF's structure-TMD system will be exactly the same as for the main mass and damper responses, respectively, in a SDOF structure-TMD system.

In other words, the driving concept of the TMD design can be summarized as follows. The device is tuned on a single frequency and anchored to a single node so that the modal expression of Eq. (1) defines the scalar dynamic equation associated to the selected frequency and is characterized by a modal mass. In such an expression, the hanging node motion appears as the associated eigenvector component multiplied by the generalized displacement of the selected node. Since the modal mass results from a normalization such that the involved eigenvector component is just one, the SDOF equation is found once again, with the only difference that the primary mass is replaced by the modal mass adequately normalized.

2.3 The standard design of a single TMD device

In this study, two critical issues, which are not consistent with the outlined standard design procedure, are addressed:

1) when using a commercial software for the finite element analyses (FEA), the modal mass normalization is pursued toward obtaining an identity matrix;

2) when the primary system is a bridge, there are longitudinal and transversal symmetries which suggest to hang several identical devices at different points; this is especially true when the vibration to be mitigated originates locally, instead than from a global oscillation of the whole structural system.

The first aspect requires (in the absence of specific options in the FEA software) to obtain from the numerical model the mass, damping and stiffness matrices, and to work directly on them (for instance, in the Matlab environment, www.mathworks.com) to perform a suitable normalization procedure.

Due to the presence of elements of the same geometry, their vibration occurs in phase or in opposition of phase, as well as in combined modes. The TMD system becomes a multiple tuned mass damper, with devices hung in several companion points. Two situations are typically identified:

A) among the modes of interest, there is one of them which sees the mass normalization associated with a selected hanging point to produce unit entries in all the companion points;

B) among the modes of interest, there are two modes at the same frequency or at frequencies close to each other which see unit entries of the first eigenvector in one half of the companion points, while the remaining points see the unit entries in the second eigenvector.

It is worth being reminded, here, that to have an eigenvector unit entry at the TMD position is the condition to deal the problem as a SDOF. For both these cases, the normalized modal mass is easily computed starting from the model matrices within a suitable software environment, for instance Matlab. A suitable per cent of it is then distributed across all the companion positions, and the TMD parameters (which are assumed to be all identical in the different locations) are accordingly computed.

However, commercial FEA codes implement a specific normalization procedure of the modal masses which is such that their resulting values have no scientific meaning. Thus, the TMD designer does not find in the FEA results the required quantities, which can only be obtained starting from the basic structural matrices (mass, stiffness and damping). This suggested the authors to conceive and implement the following alternative procedure, which by contrast, finds all the required information in the FEA results, without an explicit writing of the model matrices and the consequent Matlab calculations.

After selecting the mode and the companion TMD hanging position, a cluster of nodes whose masses could influence the single hanging point is identified and isolated. For instance, let the vibrating structural component be a beam within two nodes where other elements concur. The middle point is likely selected as hanging point for the TMD. The problem is to estimate the portion of global mass involved. For a discretization in several elements, several nodes will be introduced and their masses are likely to contribute.

In each TMD location, one accounts for the modal masses of any single cluster. The analysis is then repeated with a rigid link connecting the hanging node to an additional node where the given added mass of the TMD device is assigned. This produces a further modal mass, whose ratio to the sum of the cluster modal masses is computed. This is once again the starting point toward the standard TMD design.

In other words, instead of computing the modal mass at the hanging node and introducing the mass damper as μ times the modal mass, the ratio μ between the nodal masses as normalized by the FEA software is considered. It is important to underline that, when this procedure is adopted, the influence of the mesh discretization on the result needs to be checked by, for example, comparing them with the ones obtained from a coarser mesh. It is also worth noting that the double modal analysis is necessary because moving to a space of transformed masses, while only the ratio between added mass and participating masses is of interest.

3. A real-case exemplification

The authors had the opportunity to install sensor devices during replicated "in situ" experimental campaigns on a timber pedestrian bridge which is located in the municipality of Trasaghis, in the province of Udine, in North-Eastern Italy. A photograph of the bridge is given in Fig. 1. Although the structural scheme of this footbridge partially resembles the one of a "cable-stayed bridge", in this specific case the steel cables are replaced by two couples of long tubular steel elements. Each of the two couples is anchored to one of the two masts located on the opposite sides of the crossed channel (Fig. 1).

3.1 Geometry and materials data

The bridge span is 83 m and the deck width is 3.82 m, with 3.22 m of free crossing width. Glued laminated timber (GLT) of high strength GL28c is used for all the main structural timber elements, while glued laminated timber of strength GL24c is chosen for the walking deck. All the steel elements are made of the same material of strength S355JR. The two curved beams laterally bounding the deck have a cross-section of 0.20 by 1.941 m, and are mounted on neoprene supports at each end. They are transversally linked each to the other by a sequence of "H" shaped connectors made of tubular steel elements. These elements support five longitudinal timber beams on which the walking deck is mounted and fixed by high-strength screws. On both sides of the footbridge, the lateral beams are anchored, at their thirds, to the steel mast by means of the two aforementioned oblique tubular steel elements (not cables!) of external diameter 273 mm and thickness 8 mm. The height of the masts (Fig. 1) is about 15 m, and they are made by elements of hollow steel section of external diameter 457.5 mm and thickness 14.2 mm. It is worth noticing that the designer solution of replacing cables by rather stiff elements make the adoption of dampers ineffective since the relative velocities are lower than the threshold of effectiveness of such dampers.

3.2 Numerical modelling

In order to build a numerical model of the system, a Finite Element discretization is implemented within the Mentat-Marc (www.mscsoftware.com) software environment. A synthesis of the mass distribution along the footbridge is given in Table 1.

The numerical model is built, calibrated, and validated based on the results of two in situ experimental campaigns (Bortoluzzi *et al.* 2013a, Bortoluzzi *et al.* 2013b, Chen *et al.* 2015). In particular, the actual behavior of the joint between the tubular stays and the deck is identified (see Casciati *et al.* 2013a for the details) and the suitable material features (Casciati *et al.* 2013b) are assigned to fit the response time histories collected during the experimental campaigns. The agreement between the test records and the numerical results ensures the reliability of the adopted numerical model.

The long span feature suggested the designer to equip the timber footbridge with a supporting steel skeleton, which resulted to be quite flexible and dominant on the dynamic response of the bridge. The recorded signals confirmed the predominant role of the long tubular stays in determining the vibration of the system at frequencies in the range from 1 to 2 Hz. Actually, as a result of the modal analysis carried out on the numerical model, the possible combinations of their vertical (in plane) movements correspond to the lowest frequency value, and those of their horizontal (out-of-plane) movements correspond to an intermediate frequency range; they both induce modest movements of the deck. This different orthogonal behavior is due to the connections of the stays, which are represented by hinges in the vertical plane, but can transfer the moments in the orthogonal plane. A further slightly higher frequency sees the movement of all the oblique elements in the same (transversal/out-of-plane) direction resulting in a torsion of the central third of the deck (Table 2). A graphical representation of these modes is skipped, since it would require too many figures to cover a slight motion of the deck coming with the first mode of each of the four stays, both in-plane and out-plane, to be coupled either in phase or in opposition of phase.

The experimental damping properties are fitted by identifying the Rayleigh's coefficients, $\alpha = 0.1681$ and $\beta = 11.63\text{e-}5$, for the damping matrix of the two main GLT beams. Direct estimation of the modal damping values (which result of a mere 1% in both the two basic modes) is an alternative way which is often followed in the modelling process, especially when one preliminarily knows which are the most significant modes.

Beam and shell elements are used to generate the FE model. The numerical model of the whole bridge is shown in Fig. 2. The response to wind excitation is investigated with focus on the cases in which the vibrations are of no importance for the bridge safety, but significant enough when the user comfort is considered.

Fig. 1 Lateral view of the pedestrian timber bridge

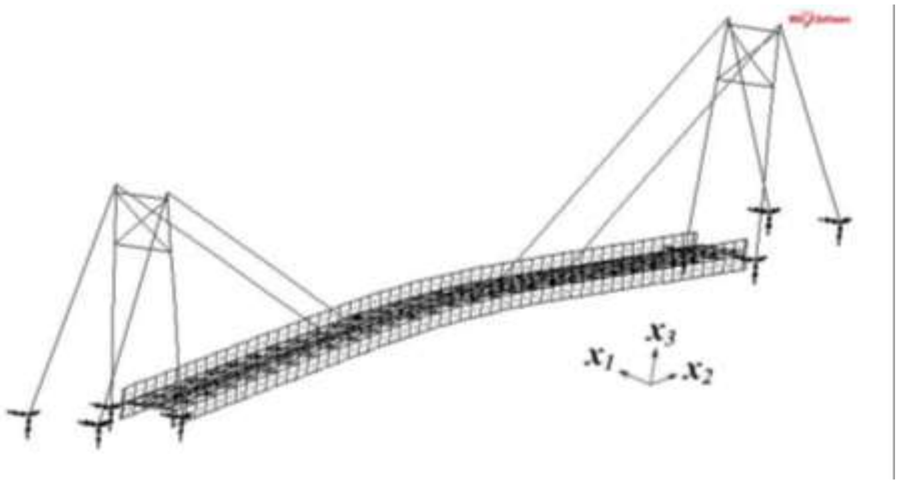

(a)

(b)

Fig. 2 (a) 3-D view of the FEM implemented in Mentat-Marc and (b) Top view of the deck

Table 1 Masses of the structural and non-structural elements

System component	*Single element mass[Kg]*	*Number of elements*	Mass [Kg]
Larch revetment	-	-	11051
GLT main longitudinal beams	16140	2	32880
Wooden walking surface	-	-	7730
Timber beams under the walking surface	828	5	4140
“Internal” tubular steel stays	1760	4	7040
“External” tubular steel stays	845	4	3380
Steel pillars	6270	2	12540
Steel railing	-	-	1200
Steel bracings	-	-	3365
Steel transversal beams	169.7	30	5090
TOTAL			**88416**

Table 2 Frequency ranges for the lowest modes. The modal analysis is performed in Mentat-Marc (www.mscsoftware.com) environment

Set ID	*Frequency [Hz]*	Involved Elements	Oscillation plane
1	1.06	Tubular stay	$x_2 - x_3$
2	1.41	Tubular stay	x_2 - x_1
3	1.96	Tubular stay	x_2 - x_1 & $x_2 - x_3$

3.3 Simulation of realizations of the wind-velocity field

Let x_2 x_3 be the plane view used for the simulation, where the axis x_2 is oriented along the deck of the footbridge, and the axis x_3 coincides with the gravity axis. The wind velocity **V** is usually idealized as the sum of two components: the "mean" part (**U**), assumed constant along an appropriate time interval, and the fluctuating part (**u**), due to the atmospheric turbulence, modeled in each point as a stationary zero mean Gaussian random process. The wind velocity field is given by

$$\mathbf{V}(\mathbf{x},t)=\mathbf{U}(x_3)+\mathbf{u}(\mathbf{x},t), \tag{6}$$

where

$$\mathbf{U}(x_3)=\frac{1}{k}\ln\left(\frac{x_3}{z_0}\right)\mathbf{e}, \tag{7}$$

Indeed, near the ground, within the inner boundary layer, the mean wind velocity has constant direction identified by the unit-vector **e** and, for a neutral stratification condition, it assumes a logarithmic profile in which k=0.41 is the Van Karman constant (Solari *et al.* 2006), z_0 the roughness length, and u* the friction velocity.

Thus, three parameters have to be defined: z_0, u*, and the time step Δt by which the simulation time axis is discretized. This last parameter was chosen to be Δt = 0.05 sec. as a compromise between achievable accuracy and required computational effort. The duration of the simulated time history is assigned to be 60 sec. in view of the exemplification purpose of these analyses. Of course, in the actual design process, longer durations would be better recommended.

Concerning the remaining two parameters, the Italian code (NTC 2008) prescriptions are adopted. Assuming u*=7 m/s, z_0 = 0.30 m, and $\mathbf{U}(x_3) = U(x_3)\ \mathbf{e_1}$, where $\mathbf{e_1}$ is the unit-vector along the axis x_1 (orthogonal to x_2 x_3), one achieves an average value of $U(x_3)$ equal to about 27 m/s for the footbridge under study.

In order to discretize the random field, one has to introduce the points of interest along the footbridge profile. In these points a wind velocity time history is then simulated. For the structure under study 23 nodes are selected, as shown in Fig. 3. In particular, eight nodes cover the masts and the oblique steel tubular elements; while the remaining fifteen nodes are equally spaced along the deck.

The simulation scheme adopted in this paper follows the references Deodatis (1996), Solari and Picardo (2001), Shinozuka and Jan (1972) and Ubertini (2010). The "weighted amplitude waves superposition" (WAWS) is used to simulate the fluctuating part. The procedure is summarized in the flow-chart of Fig. 4. A realization of the simulated time histories of the wind velocity components in the two directions along x_1 and x_3 is plotted for node *n1* in Fig. 5.

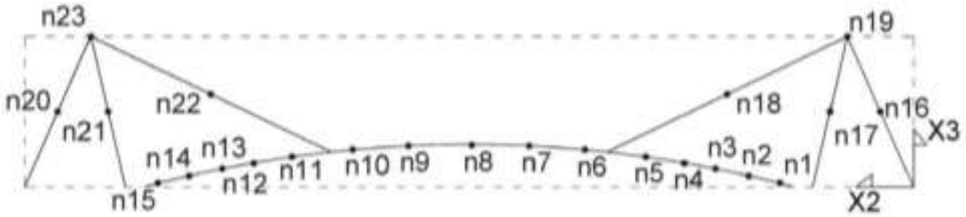

Node ID	x_2 [m]	x_3 [m]	Node ID	x_2 [m]	x_3 [m]
1	12.47	1.79	**12**	77.07	2.67
2	18.33	2.08	**13**	82.94	2.38
3	24.20	2.38	**14**	88.81	2.08
4	30.07	2.67	**15**	94.67	1.79
5	35.95	2.96	**16**	4.63	9.39
6	41.82	3.25	**17**	10.52	9.64
7	47.70	3.45	**18**	24.81	9.75
8	53.57	3.52	**19**	9.26	16.28
9	59.44	3.45	**20**	102.51	9.39
10	65.32	3.25	**21**	96.62	9.64
11	71.19	2.96	**22**	82.34	9.75
			23	97.88	16.28

Fig. 3 Grid of nodes for wind velocity field simulation

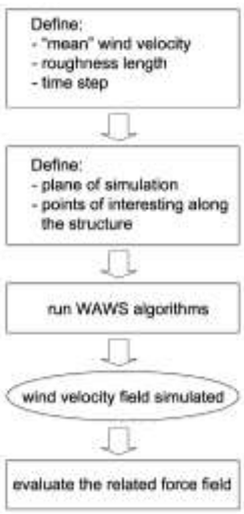

Fig. 4 Flowchart for the wind velocity field simulation

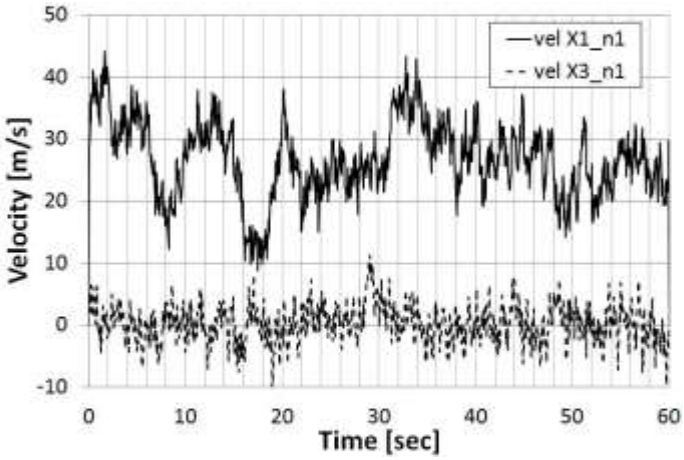

Fig. 5 Wind velocity components along the x_1 and x_3 axes as simulated for node *n1*

Once the wind velocity is obtained, standard formulae provide the values of the forces in the nodes. When introducing the time histories as boundary conditions in the finite element analyses, one can either consider them as instantaneously applied (with consequent impact phenomena), or smooth them by applying an initial and a final linear ramp (to avoid these impact phenomena). The second option is adopted in the reported simulations.

3.4 Finite Element Analysis results

The resulting forces of different intensity act on both sides of the footbridge, as prescribed in NTC (2008). Two different numerical analyses are performed:

- structural "static" analysis, from which the baseline for the dynamic vibration is obtained;
- structural "dynamic transient" analysis.

Subtracting the "static" response from the "dynamic" one in terms of displacements, it is possible to isolate the pure dynamic response of the pedestrian bridge. As an example, the displacement and accelerations time histories evaluated for the node *n22* in the transversal and vertical directions are shown in Fig. 6. The time duration of the analysis is assigned to be 120 sec; i.e., twice the duration of the wind velocity time history. In this manner, the free vibrations of the system, once the external excitation stops, are also simulated.

4. The TMD design and its performance

4.1 Details on the TMD design

In the case under study, the deck dynamics results from the stiff longitudinal timber beams, while the steel supporting skeleton is rather flexible. In particular, the values around 1 Hz of the frequencies of the modes along x_3 and x_1 (see Table 2) are associated to all the central nodes of the stays, which move in a synchronous manner (first mode of the stay, as said). This observation suggests to append the TMD directly to the middle point of the tubular steel stays (see Fig. 7(a)).

The selected tuning frequency is equal to 1.05 Hz for the motion along the x_3 (gravity) axis, and 1.40 Hz for the motion along the x_1 (transversal to the deck) axis. The values are slightly lower than those in Table 2; indeed, they account for the reduction of frequency introduced by adding mass.

In section 2 it was emphasized that the standard design of the TMD requires computational developments from the structural matrices which can be easily carried out within the software environment Matlab. The FEA model of Fig. 2 is characterized by 500 nodes and mixes beam and shell elements in order to fit not only the frequencies in Table 2 but also the higher ones. To cover the low frequencies only, a 200-nodes model is accurate enough and makes the structural matrices more manageable.

The modal mass associated to the vertical mode is found to be 4000 kg, with 1000 kg in each of the four stay central nodes. For μ=0.05, the added mass would then be 50 kg per stay.

For the mode in the horizontal direction, the reduced model yields to a decoupling of two very close frequency values, so that only two nodes move synchronously (with unity displacement). In this case, a modal mass of 1800 Kg is found and must be divided by the number of synchronous nodes (i.e., by 2), leading to 900 Kg each. For μ=0.05, the added mass would then be 45 Kg.

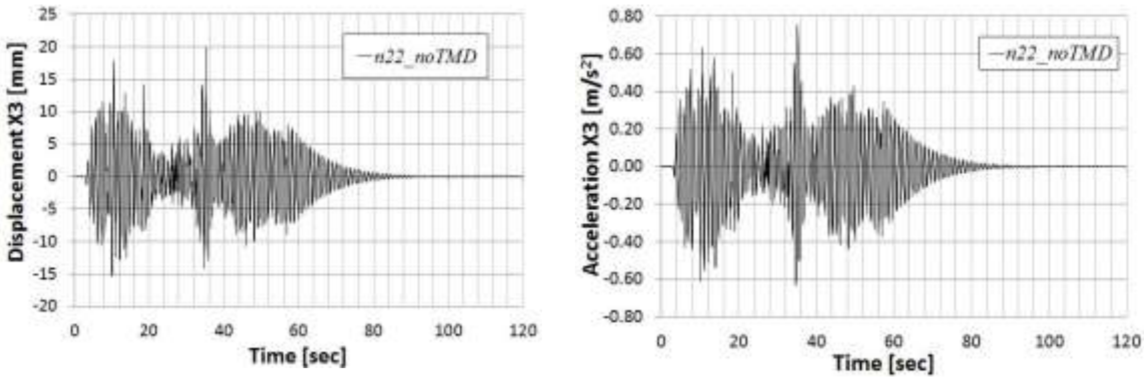

(a)

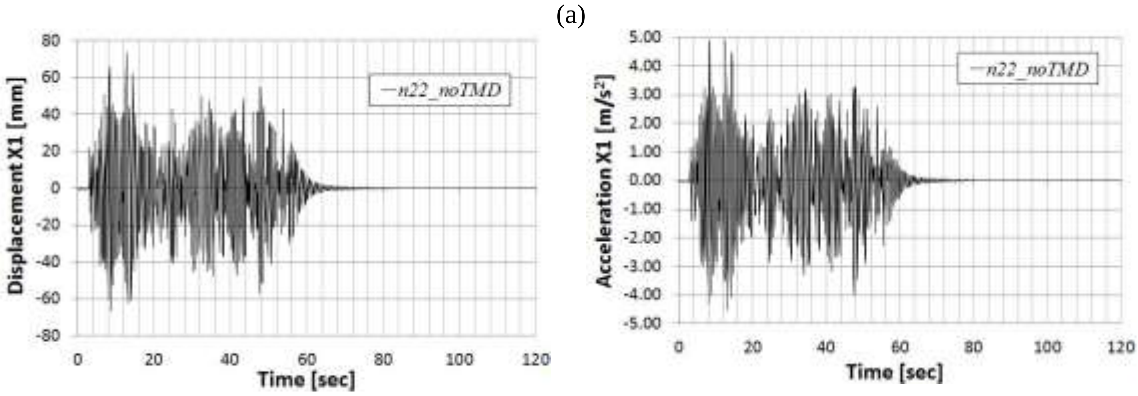

(b)

Fig. 6 Node *n22*: (a) Displacement and acceleration response along the vertical axis (x_3 axis) and (b) Displacement and acceleration response along the transversal axis (x_1 axis)

Eventually, the TMD suitable mass is derived to be 50 Kg and is applied at each stay central node, having set μ=0.0556 for the mode in the horizontal direction. It is worth noticing merly using the data in Table 1 provides a stay mass of 1760 kg. The added mass of 50 kg would therefore result in a misleading value of μ of 0.0284.

When adopting the table (7.3, page 236) for the TMD design given in Abe and Fujino (1994), one enters with the selected μ value and a very low damping of the primary system (of about 1%, which represents a conservative value of damping for wood structures) and obtains, for the motions along x_3 and x_1, stiffness values of 1950 N/m and 3400 N/m, respectively, and damping coefficients of 60 Ns/m and 80 Ns/m, respectively, thus resulting in a device damping ratio of 10%.

The alternative design approach suggested in this paper works on the large FEA model and consists of the following steps:

1) The sub-system whose vibrations have to be mitigated is first identified. In the considered case study, it is represented by the four tubular stays of total mass 1760 Kg (see Table 1). Each stay is discretized into four hollow elements leading to a nodal mass of 440 Kg per node. For further calculations, the attention is focused on the three internal nodes.
2) When considering the mode at 1.05 Hz and a rigid link to the added mass, the modal analysis provides the following (dimensionless) modal masses: 3.22, 6.55 and 4.52 for the three internal nodes, respectively, and 0.77 for the added mass. These values correspond to μ= 5.39%; the error is 7% with respect to the “lightest” FE mesh, and it will be seen to be dependent on the discretization.
3) For the mode at 1.40 Hz and a rigid link to the added mass, the modal analysis provides the following (dimensionless) modal masses: 4.09, 7.31 and 4.12 for the three internal nodes, respectively, and 0.87 for the added mass. The resulting value of μ is 5.61%, with an even lower error with respect to the “lightest” FE mesh.

Thus it is seen that the alternative approach leads to consistent results within a suitable degree of approximation. If the reasoning is repeated with a model in which the stays are just discretized into two elements, one obtains higher over-estimations of the values of μ; namely, 0.75 and 0.76 in the two directions x_3 and x_1, respectively.

Further implementation details about the proposed TMD’s solution are summarized in Figs. 7(b)-(d).

4.2 Passive control performance

The performance of the proposed TMD architecture in Fig. 7, denoted as “TMD_A”, is evaluated by computing the root mean square values of the acceleration and displacement time histories obtained at nodes *n8* and *n22* of Fig. 3 in both the directions x_1, x_3. Some examples of the analyzed time histories are plotted in Figs. 8 and 9, respectively. The calculations are carried out by considering both the whole duration of these signals and only their tails (after the 60 sec. of wind excitation); the results are reported in Tables 3 and 4, respectively.

A significant mitigation of the vibrations is achieved at the central node, *n22*, of the l.h.s stay, whereas at the deck node, *n8*, only the free response seems to be reduced. Indeed, when the entire duration of the signals at node *n8* is considered in the calculations, the devices seem to be only able to reduce the peaks in terms of both acceleration and displacement, not the root mean square values. Nevertheless, from the response of node *n8* it is evident that the addition of the stay TMDs is not deteriorating the deck performance.

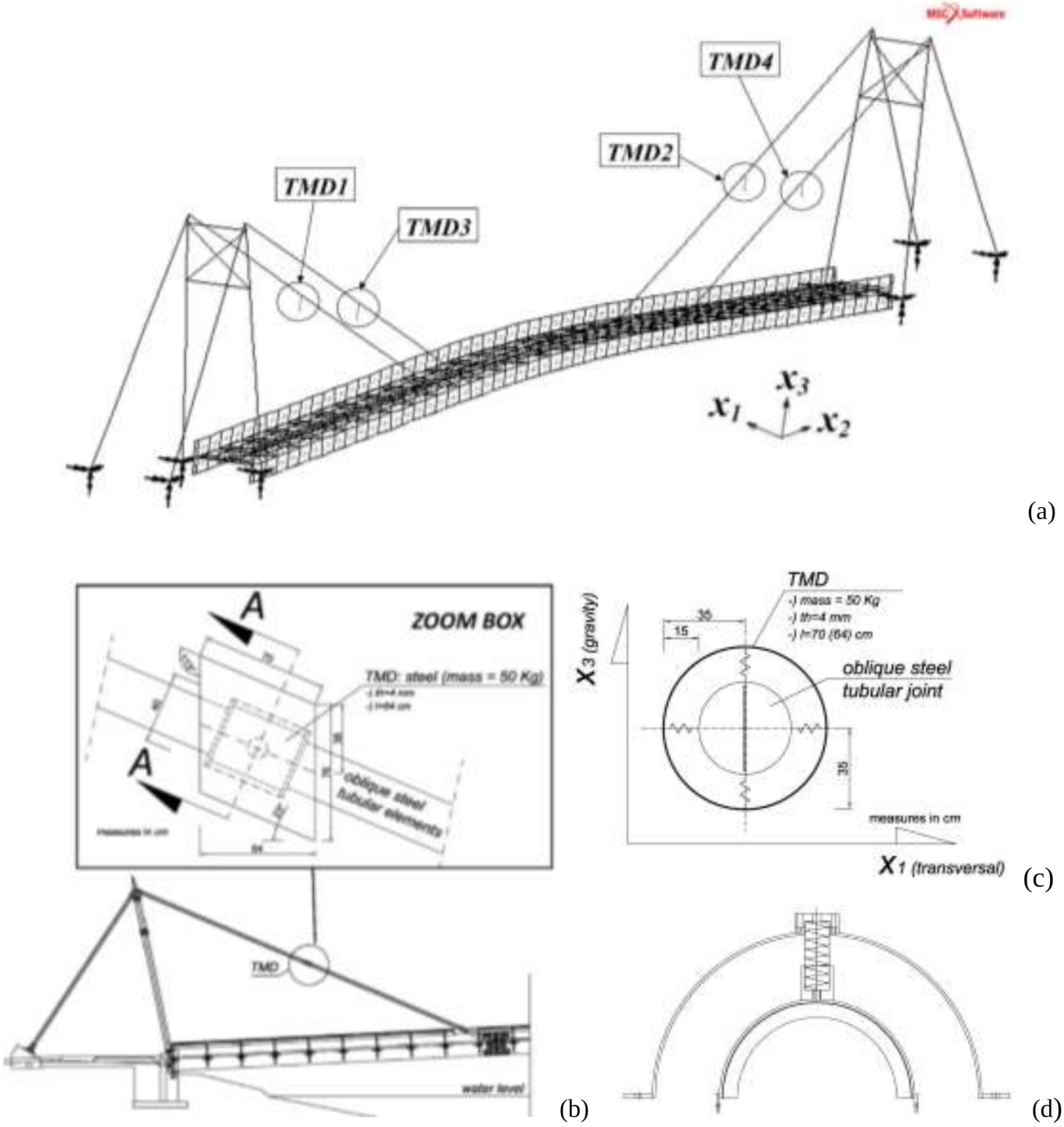

Fig. 7 (a) View of TMD1 and TMD3 hung on the tubular elements in the l.h.s. of the footbridge, and view of TMD2 and TMD4 hung on the tubular elements in the r.h.s. of the footbridge, (b) Lateral view of the location of the *i*-th TMD, (c) Cross-section of the *i*-th TMD and (d) Construction detail of the *i*-th TMD

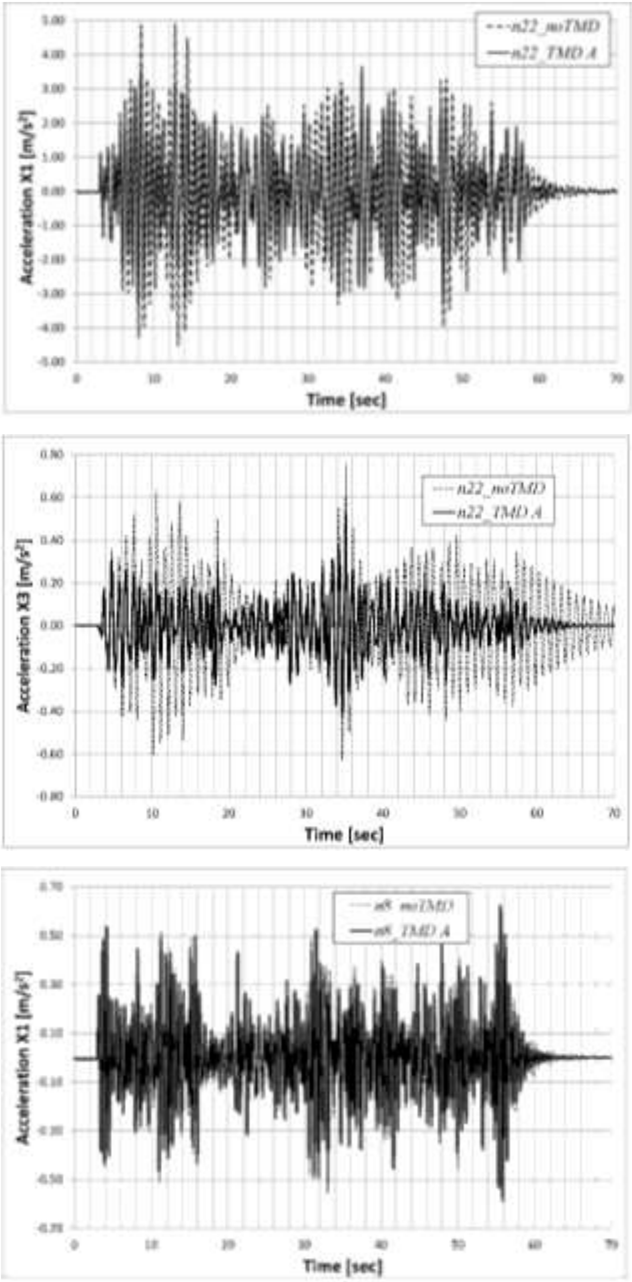

(a)

(b)

(c)

Fig. 8 Response time histories as obtained before and after mounting the passive control system denoted as "TMD_A". Zoom between 0 to 70 sec of the acceleration responses for the node *n22* along x_1 (a) and x_3 (b), respectively; (c) acceleration along x_1 at the node *n8*

Table 3 Root mean square values computed on the whole duration (120 sec) of the acceleration and displacement time histories obtained from the numerical analyses. The peak values are also reported in *italic*, and they are expressed in "m/s^2" for the accelerations, and in "mm" for the displacements

	node n8			
	acceleration		*displacement*	
	x_1	x_3	x_1	x_3
No TMD	0.1348 *0.6079*	0.0665 *0.3503*	1.2015 *5.8083*	0.5593 *2.7658*
TMD_A	0.1335 *0.6217*	0.0659 *0.3571*	1.1754 *5.9399*	0.5467 *2.8283*

	node n22			
	acceleration		*displacement*	
	x_1	x_3	x_1	x_3
No TMD	1.089 *4.8971*	0.1605 *0.7539*	15.8961 *73.4899*	3.8396 *19.8873*
TMD_A	0.8296 *3.6528*	0.0822 *0.5396*	12.7703 *58.4994*	1.9309 *14.0121*

Table 4 Root mean square values computed on the tails (the first 15 sec after the event) of the of the response time histories obtained from the numerical analyses. The peak values are also reported in *italic*, and they are expressed in "m/s^2" for the accelerations, and in "mm" for the displacements

	node n8			
	acceleration		*displacement*	
	x_1	x_3	x_1	x_3
No TMD	0.0108 *-0.0121*	0.1174 *0.0896*	0.1405 *0.1686*	0.0669 *0.0580*
TMD_A	0.0058 *0.0011*	0.0597 *-0.2571*	0.0513 *0.1547*	0.0239 *0.0735*

	node n22			
	acceleration		*displacement*	
	x_1	x_3	x_1	x_3
No TMD	0.0051 *-0.0059*	0.1014 *0.0883*	1.5997 *0.6423*	2.4365 *0.2851*
TMD_A	0.0027 *0.0012*	0.0113 *0.0275*	0.9543 *0.2421*	0.2498 *0.1143*

A further understanding of the effects of the TMD is achieved in the frequency domain by analyzing the results summarized in Figs. 10 and 11. These figures clearly confirm the above observations about the TMD's effect in terms of vibrations mitigation. In fact, by looking at the frequencies considered in the design of the TMD's (namely, 1.05 and 1.40 Hz), it is seen that the designed TMD's solution is able to smooth the spectral peaks for both the acceleration and displacement signals obtained from the numerical simulations. These observations are evident for the central node, *n22*, of the l.h.s. stay, whereas the TMD's effects are not so significant for the deck node *n8*, as already underlined above.

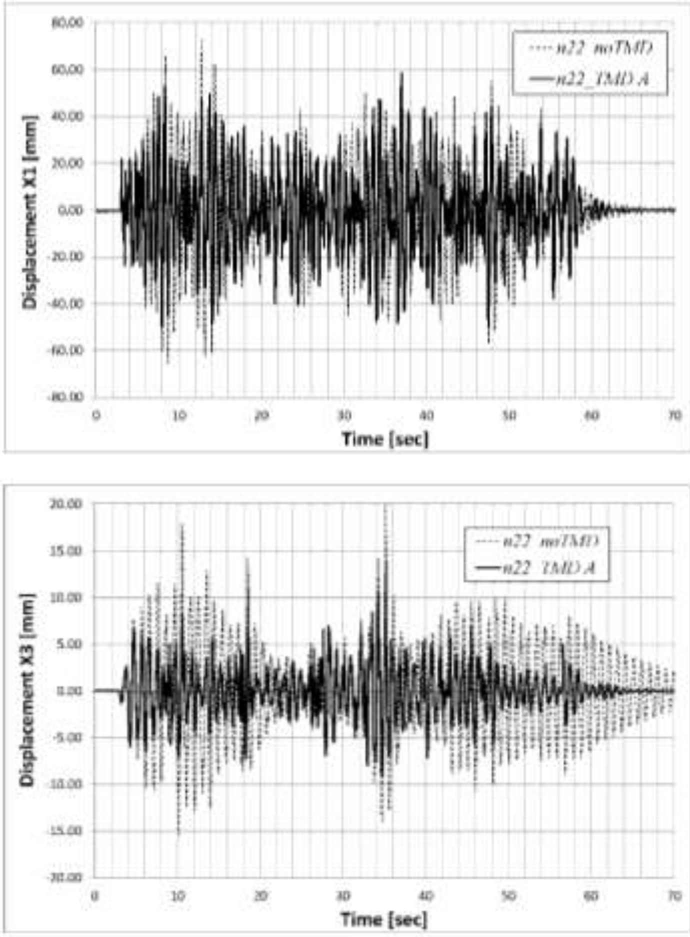

(a)

(b)

Fig. 9 Response time histories as obtained before and after mounting the passive control system denoted as "TMD_A". Zoom between 0 to 70 sec of the displacement responses for the node *n22* along x_1 (a) and x_3 (b), respectively

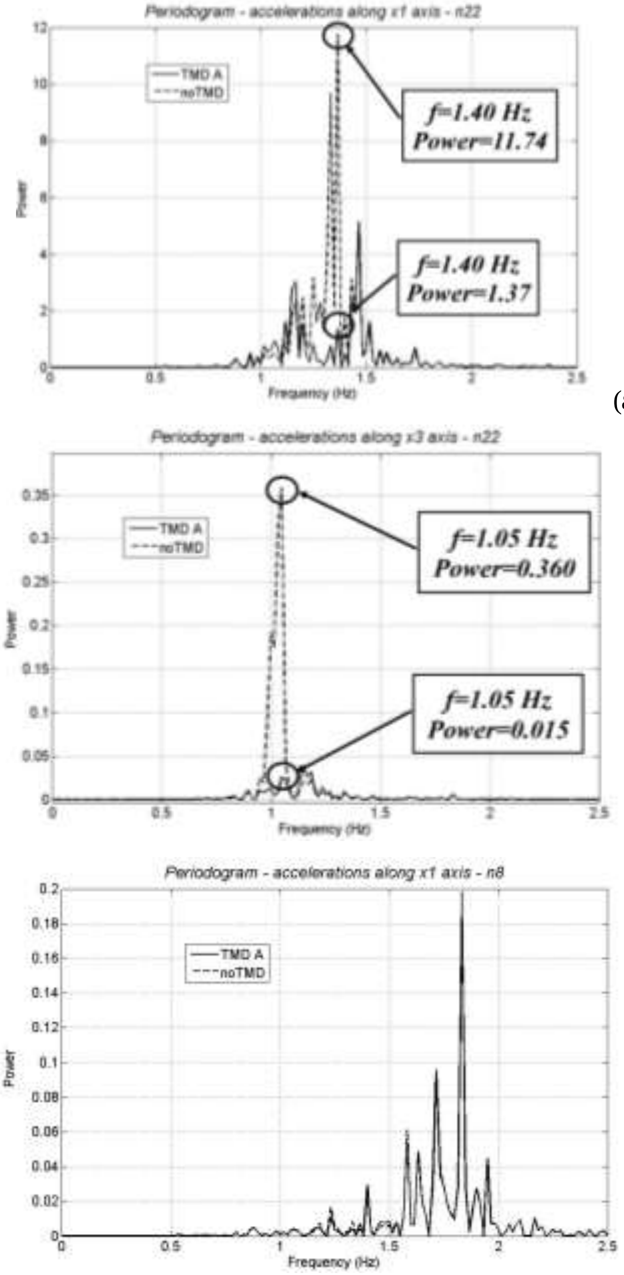

(a)

(b)

(c)

Fig. 10 Response spectra as obtained from the acceleration responses along x_1 (a) and x_3 (b) at the node *n22*; and (c) from the acceleration response along x_1 at the node *n8*, before and after mounting the passive control system denoted as "TMD_A"

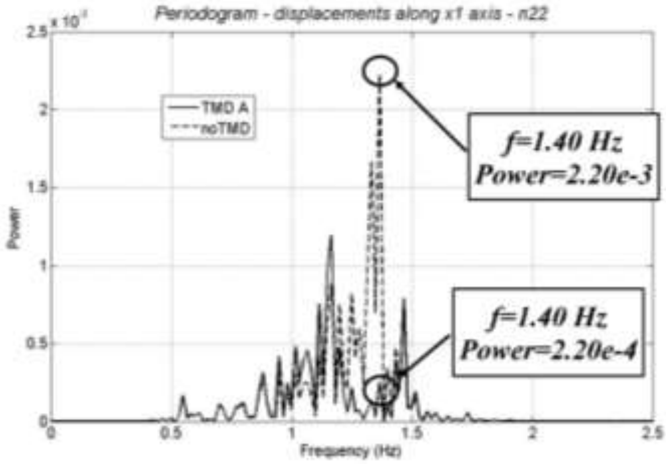

(a)

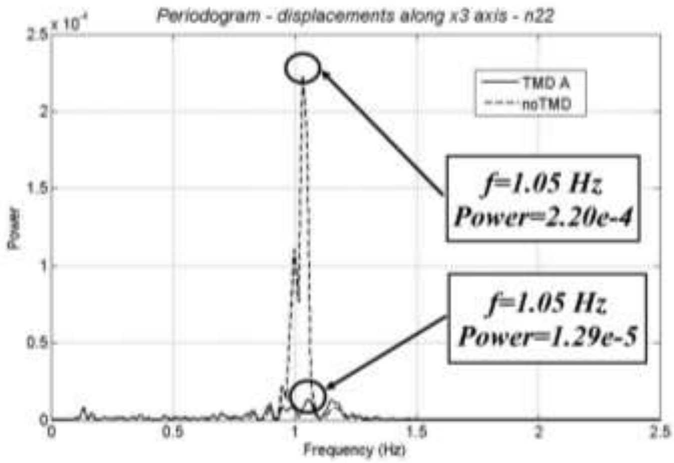

(b)

Fig. 11 Response spectra as obtained from the displacement responses along x_1 (a) and x_3 (b) at the node *n22*; before and after mounting the passive control system denoted as "TMD_A"

5. Conclusions

This paper investigates the potential of passive control solutions to mitigate the vibrations induced by the wind excitation on a slender timber footbridge. It is seen that, for a single structural mode, a passive solution based on tuned mass dampers (TMD's) results quite adequate when local rather than global oscillations are considered. The way in which standard studies (Abe and Fujino 1994) on the coupling of a secondary mass with a single degree of freedom system can be exploited when dealing with a large structural system is discussed. Mainly the potential offered by commercial finite element software tools is shown to be fully satisfactory in view of the TMD design. The explicit analysis is then numerically performed for an existing case study. Of course, full validation could only be achieved by installing the control devices on the footbridge and testing them under severe wind conditions. Further investigations could usefully address the potential of alternative active and semi-active control schemes (Casciati *et al.* 2007).

Acknowledgments

The authors are indebted with the bridge designer, Stefano Boranga, and the timber elements producer company, Rubner Holzbau S.p.A. Bolzano (Italy) for making all the technical documents available. The authors are also grateful to the Municipality of Trasaghis for the kindness shown when hosting the "in situ" experimental campaigns.

References

Abe, M. and Fujino, Y. (1994), "Dynamic characterization of multiple tuned mass dampers and some design formulas", *Earthq. Eng. Struct. D.*, **23**(8), 813-835.

Abe, M. and Igusa, T. (1995), "Tuned mass dampers with closely spaced natural frequencies", *Earthq. Eng. Struct. D.*, **24**, 247-261.

Bandivadekar, T.P. and Jangid, R.S. (2012), "Mass distribution of multiple tuned mass dampers for vibration control of Structures", *Int.J. Civil Struct. Eng.*, **3**(1), 70-84.

Bortoluzzi, D., Casciati, F., Casciati, S., Chen, Z. and Faravelli, L. (2013a), "Reporting the results of two experimental campaigns on a pedestrian timber bridge", *Proceeding of the 9th International Workshop on Structural Health Monitoring 2013 - IWSHM2013*, Stanford, California USA, September 10-12.

Bortoluzzi, D., Casciati, F., Casciati, S. and Faravelli, L. (2013b), "Comparison of accelerometric response records on a timber footbridge", *Proceeding of the 2nd International Conference on Timber Bridges 2013 – ICTB2013*, Las Vegas, Nevada USA, September 30 - October 2.

Casado, C.M., Diaz, I.M., de Sebastian J., Poncela, A.V. and Lorenzana, A. (2013), "Implementation of passive and active vibration control on an in-service footbridge", *Struct. Control Health Monit.*, **20**(1), 70-87.

Casciati, F. and Giuliano, F. (2009), "Performance of Multi-TMD in the towers of suspension bridges", *J. Vib.Control*, **15**(6), 821-847.

Casciati, F., Magonette, G. and Marazzi, F. (2007), *Technology of Semiactive Devices and Applications in Vibration Mitigation*, John Wiley & Sons, Chichester, UK.

Casciati, S. and Domaneschi, M. (2007), "Random imperfection fields to model the size effect in laboratory wood specimens", *Struct. Saf.*, **29**(4), 308-321.

Casciati, S., Faravelli, L. and Bortoluzzi, D. (2013), "Pedestrian timber bridges: experimental investigation and modeling", *Proceeding of the 10th International Conference on Damage Assessment of Structures - DAMAS2013*, Dublin, Ireland, July 8-10.

Casciati, S., Faravelli, L. and Bortoluzzi, D. (2013), "Human induced vibrations in a pedestrian timber bridge", *Proceeding of the 4th International Conference on Computational Methods in Structural Dynamics & Earthquake Engineering - COMPDYN2013*, Kos, Greece, June 12-14.

Chen, Z., Casciati, S. and Faravelli, L. (2015), "In-situ validation of a wireless data acquisition system by monitoring a pedestrian bridge", *Adv. Struct. Eng.*, **18**(1), 97-106.

Deodatis, G. (1996), "Simulation of ergodic multivariate stochastic processes", *J. Eng. Mech. - ASCE*, **122** (8), 778-787.

Diaz, I.M., Pereira, E., Hudson, M.J., Reynolds, P. (2012), "Enhancing active vibration control of pedestrian structures using inertial actuators with local feedback control", *Eng. Struct.*, **41**, 157-166.

Giordano, G., Ceccotti, A. and Uzielli L. (1999), *Tecnica delle Costruzioni in Legno* [in Italian], Hoepli,

Milano, Italy.
Moutinho, C., Cunha, A. and Caetano, E. (2011), "Analysis and control of vibration in a stress-ribbon footbridge", *Struct. Control Health Monit.*, **18**(6), 619-634.
MatLab - www.mathworks.com
MSC - http://www.mscsoftware.com
NTC (2008), *Norme tecniche per le costruzioni* (in Italian) - D.M. 14 Gennaio 2008, Italy.
Occhiuzzi, A., Spizzuoco, M. and Ricciardelli, F. (2008), "Loading models and response control of footbridges excited by running pedestrians", *Struct. Control Health Monit.*, **15**(3), 349-368.
Rana, R. and Soong, T.T. (1998), "Parametric study and simplified design of tuned mass dampers", *Eng. Struct.*, **20**(3), 193-204.
Reynders, E., Degrauwe, D., De Roeck, G., Magalhaes, F. and Caetano, E. (2010), "Combined experimental-operational modal testing of footbridges", *J. Eng. Mech . - ASCE*, **136**(6), 687-696.
Sétra Technical guide (2006), *Assessment of vibrational behavior of footbridges under pedestrian loading*, Association Française de Génie Civil, Paris, France.
Shinozuka, M. and Jan, C.M. (1972), "Digital simulation of random processes and its applications", *J. Sound Vib.*, **25**(1), 111-128.
Solari G. *et al*. (2006), "Monte Carlo simulation of wind velocity fields on complex structures", *J. Wind Eng. Ind. Aerod.*, **94**(5), 323-339.
Solari, G. and Piccardo, G. (2001), "Probabilistic 3-D turbulence modeling for gust buffeting of structures", *Probabilist. Eng. Mech.*, **16**(1), 73-86.
Soong, T.T., Dargush, G.F. (2007), *Passive Energy Dissipation Systems in Structural Engineering*, John Wiley & Sons, Chichester, UK.
Thelandersson, S. and Larsen J. H. (2003) *Timber Engineering*, John Wiley & Sons, Chichester, UK.
Ubertini, F. *et al.* (2010), "Computer simulation of stochastic wind velocity fields for structural response analysis: comparisons and applications", *Hindawi Publishing Corporation Advances in Civil Engineering*, Article ID 749578.

FC